Molecular Crystals and Liquid Crystals
Publication details, including instructions for authors and subscription information:
http://www.tandfonline.com/loi/gmcl20

Electrodeposition of Polypyrrole/Poly(Styrene Sulphonate) Composite Coatings on Ti6Al7Nb Alloy

Cristian Pirvu [a], Mihaela Mindroiu [a], Simona Popescu [a] & Ioana Demetrescu [a]

[a] Faculty of Applied Chemistry and Materials Science, University Politehnica of Bucharest, Bucharest, Romania

Version of record first published: 28 May 2010

To cite this article: Cristian Pirvu, Mihaela Mindroiu, Simona Popescu & Ioana Demetrescu (2010): Electrodeposition of Polypyrrole/Poly(Styrene Sulphonate) Composite Coatings on Ti6Al7Nb Alloy, Molecular Crystals and Liquid Crystals, 521:1, 126-139

To link to this article: http://dx.doi.org/10.1080/15421401003715884

Mol. Cryst. Liq. Cryst., Vol. 521: pp. 126–139, 2010

ISSN: 1542-1406 print/1563-5287 online
DOI: 10.1080/15421401003715884

Electrodeposition of Polypyrrole/ Poly(Styrene Sulphonate) Composite Coatings on Ti6Al7Nb Alloy

CRISTIAN PIRVU, MIHAELA MINDROIU, SIMONA POPESCU, AND IOANA DEMETRESCU

Faculty of Applied Chemistry and Materials Science, University Politehnica of Bucharest, Bucharest, Romania

The aim of this work is to study the influence of surfactants concentration on pyrrole polimerization on Ti6Al7Nb alloy in order to improve the surface performance of such biomaterials. The electrochemical stability of the polypyrrole based composite coatings were evaluated in Hank's Balanced Salt Solution by Tafel tests, cycle voltammetry and electrochemical impedance spectroscopy (EIS). The surface analysis of composite coating type atomic force microscopy (AFM), was completed with an infrared structure evaluation. The coating properties such as electrochemical parameters, wettability and roughness can be controlled by changing the pyrrole/ poly(styrene sulphonate) polymerization ratio.

Keywords AFM; anticorrosive properties; conducting polymer; contact angle; EIS; FTIR; surfactants

1. Introduction

Titanium and Ti alloys have been used extensively in particular as *biomaterials* due to their high strength-to-weight ratio, good biocompatibility and excellent corrosion resistance [1,2].

Ti-6Al-7Nb is a titanium alloy for medical and surgical device applications with properties almost identical to Ti-6Al-4V, substituting niobium for vanadium as the beta stabilizing element. Ti-6Al-7Nb alloy is widely used in the *medical device industry*, primarily for orthopedic applications [3–5].

Modifications of titanium alloy surfaces are often used in order to improve the biological, chemical, and mechanical properties. Different surface modification methods have been used to improve surface characteristics, such as: mechanical methods (grinding, polishing [6,7]) chemical methods (acidic or alkaline treatment, CVD [8]) biochemical methods, electrochemical methods (anodic oxidation, electrochemical deposition [9–12]), physical methods (thermal spray, PVD, ion implantation and electro deposition [13]).

Address correspondence to Cristian Pirvu, Faculty of Applied Chemistry and Materials Science, University Politehnica of Bucharest, Polizu no 1–7, Bucharest 011061, Romania. Tel.: 4023930; Fax: 4021.311.17.96; E-mail: c_pirvu@chim.upb.ro

The coatings based on conducting polymers present important advantages for biomedical applications, including: biocompatibility, ability to entrap and controllably release biological molecules, chemical and electrochemical stability useful in many biomedical applications: biosensors, tissue-engineering scaffolds, neural probes, drug-delivery devices, bio-actuators [14,15].

Electrically conductive polypyrrole (PPy) has demonstrated substantial potential for biomedical application because it may be used in contact with biological components to apply an electrical stimulation and electrochemically grown directly onto metallic substrates of any shape and dimension [16,17].

The possibility of a polymer film formation directly on a metal surface in the electropolymerization process is a large advantage, thus such films are obtained mostly by the polymerization of appropriates monomers [18].

Conducting polymer coatings such as polyaniline (PAni), polypyrrole (PPy), polythiophene (PT), etc. [19–20]. have been shown to offer protection of different metals. Among these coatings, PPy presents high potential application owing to the low monomer toxicity, its high stability in oxidized state and ease of synthesis in aqueous solutions [21].

Electrodeposited PPy induced various biological application as hidroxyapatite incorporation, doped systems with species as biotin and hyaluronic acid or polymer surface modification through a graft of protein sequences able to promote a specific cellular response. It is known that pyrrole monomer is not biocompatible but cell culture on its polymer reveal good cell viability and adherence, [22–25].

Polymerization in the presence of surfactant anions have also been found to yield uniform CP films on metalic surface [26,27]. Pyrrole has a large overpotential for oxidation at the alloy surface. The apparently results from the incompatibility of the rather hydrophobic Py monomer and the rather hydrophilic alloy (oxide) surface can be minimize by using of surfactants during polymerization [28].

Electrically conductive polypyrrole-coated titanium enhanced osteoblast functions *in vitro* significantly. This novel surface modification has potential applications to improve performance of titanium implants *in vivo*.

Electropolymerization of pyrrole on titanium substrates for the future development of new biocompatible surfaces.

A wide range of molecular dopants such as DNA, antibodies, enzymes, surfactants, growth factors and even whole living cells can be to change surface biocompatibility. Aromatic and very large amphiphilic sulfonate dopants provided the best conductivities, stabilities and mechanical properties to the polymer film [29]. Large anions like PSS are interesting, because they possibly prevent ingress into the layer by aggressive anions like chloride.

The ability to control PPy's surface properties such as wettability and charge density creates the potential for modifying neural interactions with the polymer. Two of the most common dopants that are co-deposited with PPy are polystyrenesulfonate (PSS) or sodium dodecylbenzenesulfonate (NaDBS). PSS/PPy and NaDBS/PPy polymers have been used in many applications ranging from actuators to neural electrode coatings to neural substrates [30].

The present work is focused on electrochemical deposition of polypyrrole/poly(styrene sulphonate) composite coatings on Ti6Al7Nb alloy following to study the influence of surfactants concentration on pyrrole polymerization in order to improve the surface stability.

2. Materials and Methods

The substrates were represented by Ti-6Al-7Nb alloy with composition given in Table 1. All experiments were carried out on disk-shaped samples (1 cm diameter, 2 cm thickness).

Their surface was polished until a mirroring finish was achieved ($Ra = 1\,\mu m$) using silica carbide paper with up to 1200 granularity and cleaned in ultrasonic bath before performing the electrodeposition experiments.

The polypyrrole films were synthesized electrochemically from aqueous solution containing $0.2\,mol\,L^{-1}$ Py (Aldrich) purified just before use by vacuum distillation at 62°C and $0.2\,mol\,L^{-1}$ oxalic acid (Aldrich) as support electrolyte using potentiostatic method, the working electrode had been maintained for 500 seconds at 0.9 V vs. Ag/AgCl.

In order to improve the surface characteristics of the Ti alloy/PPy electrode system, a NaPSS (poli(sodium-4stryrensulfonate)) anionic surfactant with different concentrations (0.01, 0.05, 0.1, and $0.2\,mol\,L^{-1}$) have been used for the polymerization. Measurements of the corrosion behavior of coated and uncoated Ti6Al7Nb alloys were performed in aerated simulated physiological Hank's Balanced Salt Solution (HBSS) [31] containing (in gL^{-1}): 8 NaCl, 0.4 KCl, 0.35 $NaHCO_3$, 0.25 $NaH_2PO_4 \cdot H_2O$, 0.06 $Na_2HPO_4 \cdot 2H_2O$, 0.19 $CaCl_2 \cdot 2H_2O$, 0.19 $MgCl_2$, 0.06 $MgSO_4 \cdot 7H_2O$, 1 glucose, at $pH = 6.9$.

From Tafel plots the following main electrochemical parameters were calculated: i_{cor}, corrosion current density; R_p, polarisation resistance; E_{cor}, corrosion potential; V_{cor}, corrosion rate.

The EIS measurements were made at free potential in Hank solution and in frequency domain between $0.01 - 10.000\,Hz$ with amplitude by $\pm 10\,mV$ (rms). EIS analysis was discussed in term of Bode and Nyquist representations.

In order to establish the electrochemical stability of the polymeric composites obtained films, the polarization curves were performed in potential domain between $-0.5\,V$ to $+1\,V$, for 10 cycles with a scan rate of $0.05\,V/s$.

All electrochemical measurements were performed using a one compartment cell with three electrodes: a working electrode, a platinum counter-electrode and an Ag/AgCl, KCl reference electrode connected to Autolab PGSTAT 302 N potentiostat with NOVA general-purpose electrochemical system software.

The wettability tests were made used KSV Instruments LTD optical stage microscope equipped with CAM100 to record the shape of the drops and measure the contact angle.

The FTIR spectroscopic analysis for PPy and for the composites PPy/surfactants films was done by Perkin Elmer FT-IR spectrophotometer 100 using diamond ATR technique (scanning range from $4000\,cm^{-1}$ to $600\,cm^{-1}$).

In order to investigate the surface topography of PPy/surfactant composites modified surfaces the contact mode AFM was used from APE Research, Italia.

Table 1. Composition of the Ti-6Al-7Nb alloy

Element	Ti	Al	Nb	Fe	H	N	O	C
(wt% values)	rest	5.88	6.65	0.3	0.0121	0.05	0.2	0.1

3. Results and Discussion

3.1. *Electrochemical Deposition of Polypyrrole Coating*

In all cases, the current transient obtained for a typical potentiostatic PPy electrodeposition can be divided into three stages: at the beginning, the current density decreased drastically during the electrode passivation due to oxide layer formation, this period is calling the induction period; in the second stage the current density increased reaching to the maxim value (i_{max}) that means the polymer nucleation is started, and in the third stage can be observed that the current density became practically constant corresponding to the polymer electrodeposition (Fig. 1). The i_{max} and t_{max} values depends on the NaPSS concentration used in polymerisation process.

Increasing the surfactant concentration increase the i_{max} values and decrease the t_{max} values respectively, corresponding to the higher polimerization rate, the same behaviour was observed by De Giglio were the KCl electrolyte was used [32].

The polymer nucleation from aqueous monomer solution with 0.01 M NaPSS was started at $i_{max} = 0.481\,\text{mA/cm}^2$ reached after $t_{max} = 59$ seconds. When the addition of NaPSS is by 0.05 M the i_{max} and t_{max} values are $1\,\text{mA/cm}^2$ and 51 seconds respectively, in case of 0.1 M NaPSS addition the i_{max} and t_{max} values are $1.65\,\text{mA/cm}^2$ and 37 seconds and finally when the surfactant concentration is 0.2 M the i_{max} and t_{max} values are $3.22\,\text{mA/cm}^2$ and 15 seconds, respectively.

For concentrations higher than $0.2\,\text{mol L}^{-1}$ NaPSS it was observed that the PPy films are not adherent on the Ti6Al7Nb surface. This behaviour can be attributed to higher adsorption of surfactants on the electrode surface which detain the pyrrole polymerization. However, once the monomer oxidation is initiated, this process is faster for increased surfactant concentration, as shown by the increase in current density [33].

3.2. *Electrochemical and Corrosion Characterization*

3.2.1. *Tafel Plots.* The corrosion behavior of Ti alloy/PPy and Ti alloy/PPy/NaPSS modified electrodes were estimated by Tafel plots in HBSS showed in

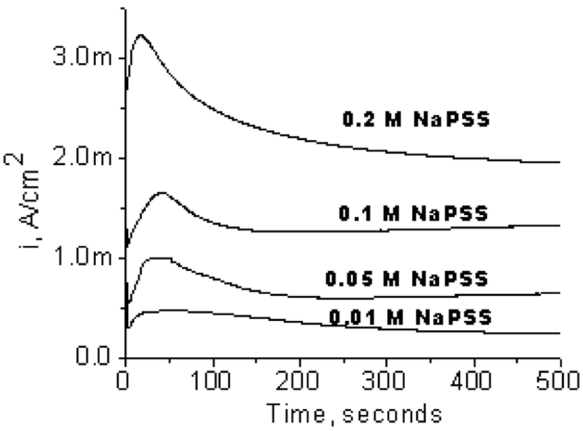

Figure 1. Potentiostatic polymerization of pyrrole using $0.2\,\text{mol L}^{-1}$ Py, $0.2\,\text{mol L}^{-1}$ Oxalic acid and different concentrations of NaPSS.

Figure 2. To substantiate the anticorrosion properties the Tafel regions of cathodic and anodic polarization curves are extrapolated.

In Table 2 are presented the corrosion parameters and polarization resistances obtained from Tafel diagrams.

This potential shift is associated with an increase of corrosion current with approximately two orders of magnitude for Ti/PPY surface comparing with titanium natural passivated surface due to replacing of low conducting TiO_2 layer with PPy conducting polymer. The corrosion rate is also increasing as can be seen in Table 2, but due to the polymer contribution, this fact is not a real reduction of stability. In the literature [34] such modifications of current densities and corrosion rate is explained based on the complex process due to several electroactive species and surfaces with structural and morphological exchanges.

In the case of NaPSS addition the variation of corrosion potential in anodic direction is not a significant one, being only 33 mV, for a concentration of 0.1 M. The Ti/PPy+NaPSS 0.1 M composite presents better stability comparing to the Ti/PPy after an adition of 10 times less of NaPSS concentration. For 0.2 NaPSS addition the corrosion rate increase and such behaviour is an argument for the idea that the dependence of corrosion rate on the surfactant concentration is depending of concentration domain. From calculated electrochemical parameters it could be seen that the presence of surfactants have a small contribution on improving of corrosion resistance, on the contrary, for lower concentration of NaPSS the corrosion current presents a minor rise probably due to improving of conductive behavior of PPy in the presence of PSS dopants. Being a conductive polymer the conductivity of PPy consists of two terms, one of them related to transport of charge carrier along the polymer chain and other one due to their transport from one chain to other chain, respectively. At higher concentration of dopants the interchain transport of charge carrier could be partially blocked [35].

However, the better anti-corrosion parameters were obtained for 0.1 mol L^{-1} concentration of NaPSS surfactant used when was obtained a higher polarization resistance, around 2 times the value for the system without surfactant. This value corresponds to the best hydrophilic surface character.

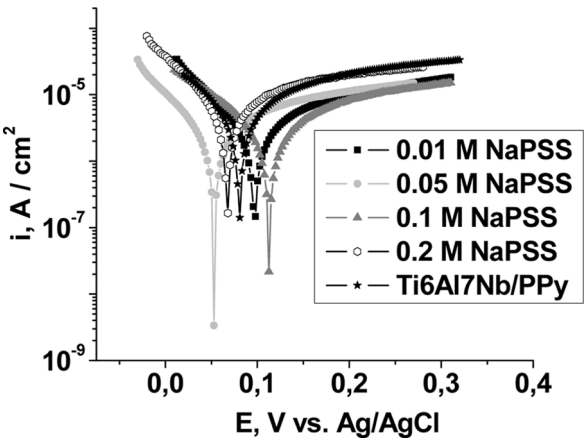

Figure 2. The polarization curves for Ti6Al7Nb/PPy and Ti6Al7Nb/PPy/surfactants electrodes in Hank' solution.

Table 2. Corrosion parameters and polarisation resistances obtained from Tafel diagrams

Electrodes	i_{cor} (A/cm^2)	R_p (Ω/cm^2)	E_{cor} (V)	V_{cor} (mm/year)
TiAlNb/PPy	$2.108 \cdot 10^{-6}$	$4.184 \cdot 10^{+3}$	0.08	$5.913 \cdot 10^{-2}$
TiAlNb/PPy/NaPSS 0.01 M	$3.618 \cdot 10^{-6}$	$2.404 \cdot 10^{+3}$	0.097	$1.091 \cdot 10^{-1}$
TiAlNb/PPy/NaPSS 0.05 M	$3.306 \cdot 10^{-6}$	$1.443 \cdot 10^{+3}$	0.053	$9.971 \cdot 10^{-2}$
TiAlNb/Ppy/NaPSS 0.1 M	$5.012 \cdot 10^{-7}$	$8.311 \cdot 10^{+3}$	0.113	$4.686 \cdot 10^{-2}$
TiAlNb/Ppy/NaPSS 0.2 M	$7.024 \cdot 10^{-6}$	$0.915 \cdot 10^{+3}$	0.067	$2.119 \cdot 10^{-1}$

3.2.2. *Electrochemical Impedance Spectroscopy (EIS).* Nyquist spectra for Ti6Al7Nb/PPy are quite similar to Ti/PPy electrode spectra doped with some anions [36], having a single semicircle for charge transfer process and a diffusion tail. The spectra of Ti6Al7Nb/PPy and Ti6Al7Nb/PPy/surfactants modified electrodes are presented in the Figure 3 for four different concentrations of surfactants.

From Nyquist plots it can be observed that the highest charge transfer resistance was obtained for 0.1 mol L^{-1} concentration NaPSS surfactant, the results being in concordance with those from Tafel plots. For other surfactants concentrations the charge transfer resistance decay with the surfactant concentration reduction. In the case of 0.2 mol L^{-1} NaPSS, the polarization resistance is lower probably because the polymeric film obtained in this case is not perfect adherent on the Ti6Al7Nb alloy substrate.

In Figure 4 the Bode spectra Ti6Al7Nb/PPy and Ti6Al7Nb/PPy/surfactants modified electrodes in Hank solution were represented. The Z Bode spectra for 0.1 mol L^{-1} concentration NaPSS surfactant have two time constants and the phase angle value is almost 80° indicating a capacitive behavior of the obtained PPy/NaPSS composite coating. Also, for 0.01 mol L^{-1} and 0.05 mol L^{-1} NaPSS doping

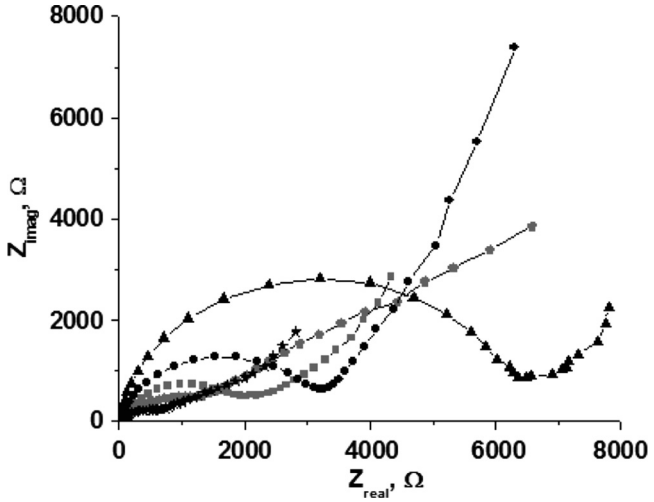

Figure 3. Nyquist spectra for Ti6Al7Nb/PPy and Ti6Al7Nb/PPy/surfactants electrodes in Hank solution.

concentrations, the Z Bode spectra have one time constant but the phase angle value is of about 45°, which suggest presence of a Warburg element due to diffusion behavior through composite coatings A special situation was observed in case of $0.2\,mol\,L^{-1}$ NaPSS concentration, were the Z Bode spectra present two time constants and almost 45° phase angle value indicating a Warburg diffusion behavior.

The equivalent electric circuits used to fit the EIS data obtained for $0.01\,mol\,L^{-1}$ and $0.05\,mol\,L^{-1}$ NaPSS concentrations (Fig. 5a), contain Hank solution resistance (R_S), charge transfer resistance (R_{CT}) in parallel bonded with double layer capacitance (CPE_{DL}) and in series bonded with Warburg diffusion coefficient (W).

In case of $0.1\,mol\,L^{-1}$ NaPSS concentration, the equivalent electric circuit (Fig. 5b) contains a supplementary constant faze (CPE_C) corresponding to the compact composite coating, indicated the capacitive behavior of this film.

On the other hand, the equivalent electric circuit proposed for $0.2\,mol\,L^{-1}$ NaPSS concentration (Fig. 5c) is different, having a Warburg diffusion coefficient, indicating diffusion processes through polymeric film. The R_C is the resistance of the composite coating in parallel bonded with constant phase element (CPE_C) corresponding to the composite coating and the (R_{CT}) and (CPE_{DL}) are charge transfer resistance and double layer capacitance respectively for Ti6Al7Nb/Hank solution interface formed due to the diffusion process through polymeric coating.

The electrical parameters obtained after fitting of proposed circuits are presented in the Table 3.

The highest polarization resistance value corresponding to the polymeric composite film was obtained for $0.1\,mol\,L^{-1}$ NaPSS doping concentration. Despite the fact that apparently the behavior can be classified as aleatory, in fact it is a trend of variation depending of the concentration domain of surfactant, as a result of surface process change.

3.2.3. *Cyclic Voltammetry.* In order to establish the electrochemical stability of the polymeric composites obtained films, the polarization curves were performed in potential domain between −0.5–1 V, for 10 cycles with a scan rate of about 0.05 V/s using a 320 Autolab potentiostat.

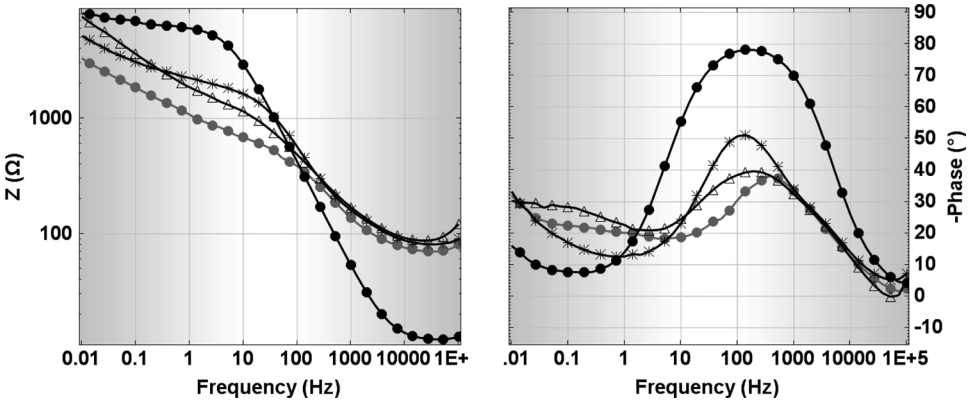

Figure 4. (a) Z Bode spectra and (b) phase angle Bode spectra for Ti6Al7Nb/PPy and Ti6Al7Nb/PPy/surfactants electrodes in Hank solution.

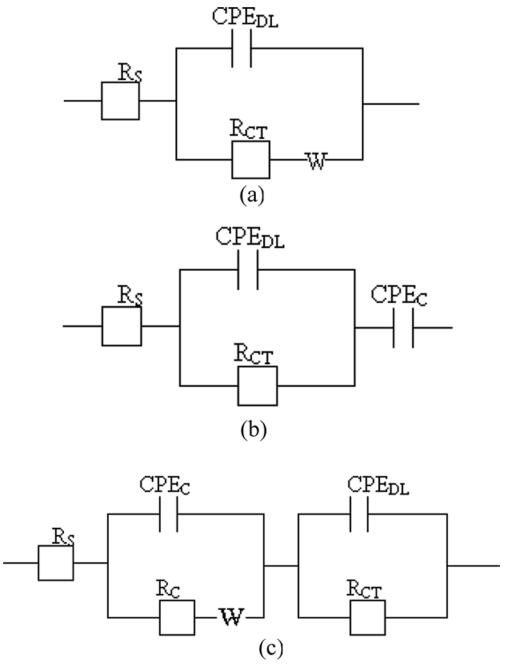

Figure 5. The electrical circuits for (a) Ti6Al7Nb/PPy/0.01 mol L^{-1} and 0.05 mol L^{-1} NaPSS; (b) Ti6Al7Nb/PPy/0.1 mol L^{-1} NaPSS and Ti6Al7Nb/PPy potentiostatically deposited; (c) Ti6Al7Nb/PPy/NaPSS 0.2 mol L^{-1} NaPSS used for fit EIS data.

Cyclic voltammograms recorded for Ti6Al7Nb/ Ppy electrode (Fig. 6a), shows a capacitive behavior and a good electrochemical stability where the ten successive cycles are practically overlaid.

However, a slow creeping phenomenon can be observed on the cyclic volatammograms. The similar result that creeping was also significant in the reduced state was reported by Madden *et al.* [37] in PPy film doped with PF_6.

The result is likely related to the fact that the stiffness of film in the oxidized state is larger than that of reduced state.

3.3. *Surface Characterization*

3.3.1. *Wettability Tests.* Contact angle measurements were carried out in order to evaluate the wettability of the surface-modified alloy as resulting of every treatment [38–39]. An equal volume of distilled water was placed on every sample by means of micropipette, forming a drop or spreading on the surface.

In the Table 4, the contact angle measurement results are presented for all samples.

The surfactant concentration added showed a great influence on the surface wettability in particular due to the presence of sulfonic hydrophilic groups, which as expected determined a shift to more hydrophilic domain. Large surfactant anions remain immobilized in the polymer matrix and are mainly involved in the changing of wettability.

Distilled water put on uncoated sample formed a regular drop, with a contact angle of about 84°. After PPy electrodeposition, the contact angle decreases to

Table 3. Electrical parameters of equivalent circuits obtained by fitting the experimental results of EIS test

Parameters	TiAlNb/PPy/ NaPSS	TiAlNb/PPy/ 0.01 M NaPSS	TiAlNb/PPy/ 0.05 M NaPSS	TiAlNb/PPy/ 0.1 M NaPSS	TiAlNb/PPy/ 0.2 M NaPSS
R_S (Ω)	22.26	79.2	82.3	11.68	67.8
CPE_{DL} (Fcm^{-2})	$0.8932 \cdot 10^{-5}$	$0.1325 \cdot 10^{-4}$	$0.3123 \cdot 10^{-4}$	$0.6204 \cdot 10^{-5}$	$0.1786 \cdot 10^{-4}$
n_1	0.8251	0.7643	0.6744	0.927	0.744
R_{CT} (Ω)	3220	1940	1269	6290	520
W	–	$0.1036 \cdot 10^{-2}$	$0.552 \cdot 10^{-2}$	–	$0.1663 \cdot 10^{-2}$
CPE_C (Fcm^{-2})	$0.9278 \cdot 10^{-3}$	–	–	$0.1866 \cdot 10^{-2}$	$0.574 \cdot 10^{-3}$
n2	0.7175	–	–	0.6206	0.7
R_C (Ω)	–	–	–	–	683

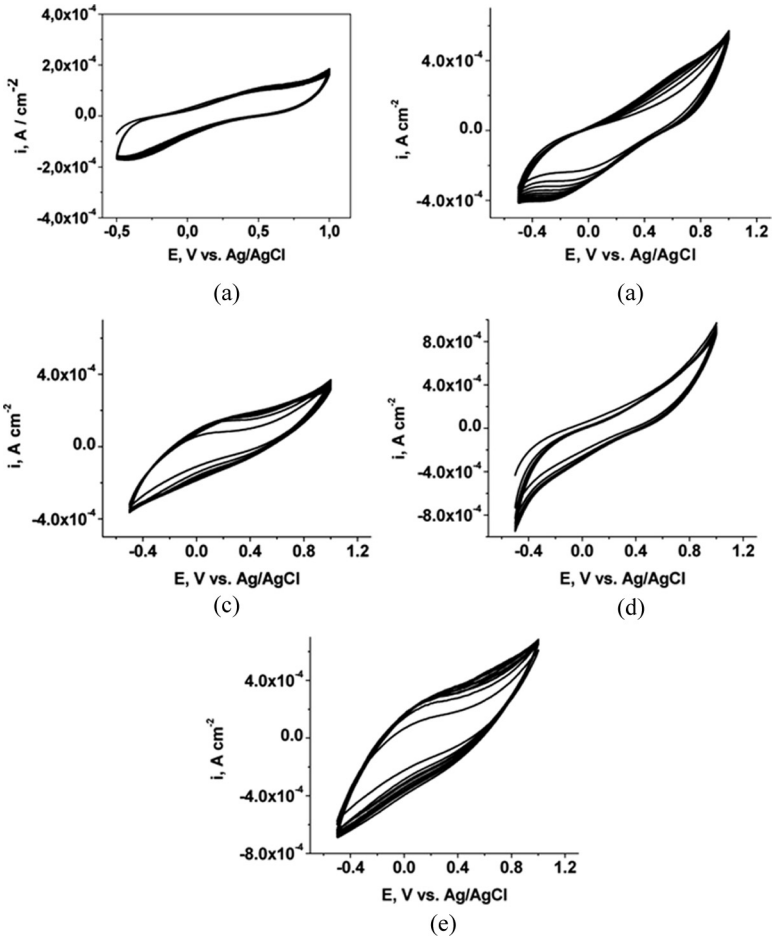

Figure 6. Cyclic voltammograms for (a) Ti6Al7Nb/PPy potentiostatically deposited; (b) Ti6Al7Nb/PPy/0.01 mol L^{-1} NaPSS; (c) Ti6Al7Nb/PPy/0.05 mol L^{-1} NaPSS; (d) Ti6Al7Nb/PPy/0.1 mol L^{-1} NaPSS; (e) Ti6Al7Nb/PPy/0.2 mol L^{-1} NaPSS.

55.96°, the surface being more easily wetted, resulting in a low contact angle. Also, the presence of surfactants decrease the contact angle values, showing a higher hydrophilic behavior than that observe in case of PPy without doping surfactants. The best hydrophilic behavior was observed in case of Ti6Al7Nb/PPy/0.1 mol L^{-1} NaPSS electrode, with the contact angle value of about 10.14°.

As a surface becomes more oxidized, or has more ionizable groups introduced to it, hydrogen bonding with the water becomes more facile and the droplet spreads along the hydrophilic surface, resulting in a lower contact angle.

The wettability of conducting polymers depends greatly on the types of dopants used.

For example, a PPy film containing a perfluorinated dopant exhibited hydrophobicity (water contact angle >90°), while ClO_4^- doped PPy was hydrophilic [40] and for PSS^- we determined an hydrophilic character (from 55° to 10°).

Furthermore, the doping level can be controlled by changing the electrical potential, resulting in reversibly switchable surface wettability [41].

Table 4. The results of contact angle and roughness measurements

Electrods	CA (contact angel) (°)	CA standard deviation	Ra, roughness average (μm)	Rms, roughness root-mean-square (μm)
Ti6Al7Nb/PPy	55.96	0.73	0.189	0.231
TiAlNb/PPy/NaPSS 0.01 M	32.09	1.73	0.340	0.413
TiAlNb/PPy/NaPSS 0.05 M	55.84	0.72	0.271	0.342
TiAlNb/Ppy/NaPSS 0.1 M	10.14	1.02	0.292	0.354
TiAlNb/Ppy/NaPSS 0.5 M	33.92	1.40	0.219	0.296

3.3.2. *The Fourier Transform Infrared Spectroscopic (FT-IR) Characterization.* The FTIR spectra for PPy and for the composites PPy/surfactants films are presented in Figure 7.

The NH stretching band of pyrrole ring which appears at 3421.38 cm^{-1} in case of PPy spectrum, also is presents on PPy/NaPSS spectrum at 3410.97 cm^{-1}. The band at 3366.51 cm^{-1} from NaPSS spectrum corresponds to the OH band. The weak bands between 2700–2000 cm^{-1} corresponds to the stretch vibration of C−H bond [42–44], observe only in PPy and PPy/NaPSS spectra. In case of spectrum for PPy obtained by potentiostatic method the absorption bands at 1621.67 cm^{-1} corresponds

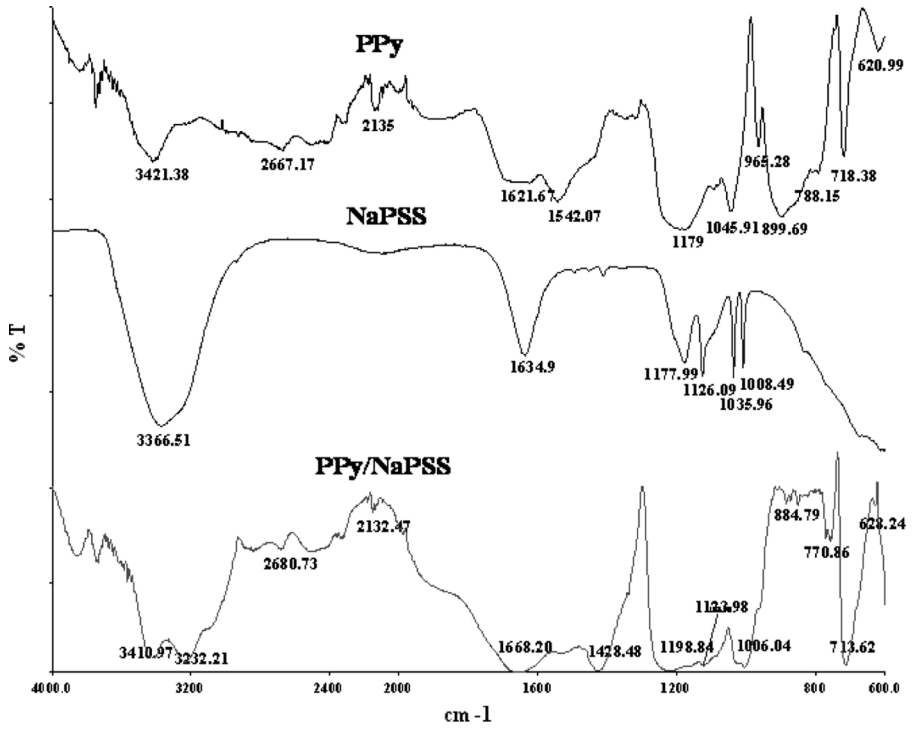

Figure 7. The FT-IR spectra of PPy and PPy/surfactants composites electrodeposited in oxalic acid aqueous solution by potentiostatic method.

to the C=C ring stretching of pyrrole which is presents in PPy/NaPSS spectrum at 1668.20 cm^{-1}. The typical polypyrrole ring fundamental N−H vibrations were observed at 1542.07 cm^{-1} in PPy spectrum and at 1428.48 cm^{-1} in PPy/NaPSS spectrum [45,46]. The C−C stretching bands are presented in PPy and PPy/NaPSS spectra at 1179 cm^{-1} and at 1198.84 cm^{-1} respectively. The bands at 1126.09 cm^{-1} and at 1008.49 cm^{-1} [47] from NaPSS spectrum are associated with the symmetric and asymmetric S=O stretch vibrations of the sulfonic group. However, these groups were observed in PPy/NaPSS spectrum at 1123.98 cm^{-1} and at 1006.04 cm^{-1}. The peaks observed in PPy spectrum at 1045.91 cm^{-1} absorption band corresponding to the =C−H in plane vibration [48] and at 965.28 cm^{-1} out of C−C stretching are not observed in case of PPy/NaPSS spectrum. But the =C−H out of plane vibration at 718.38 cm^{-1} and at 713.62 cm^{-1}, indicating the polymerization of pyrole [46] which are presented in both spectra, PPy and PPy/NaPSS respectively.

3.3.3. *Surface Analysis with Atomic Force Microscopy.* Figure 8 presents the two-dimensional images at different dimension scans of the surface for potentiostatic electrodeposition of PPy/surfactants films in aqueous electrolyte.

The $50 \times 50\,\mu m^2$ AFM images of the PPy/NaPSS surface appeared to be composed of bigger grain size with increase of NaPSS concentration showing that the concentration of the surfactant plays an important role in the electropolymerisation process.

From $1.5 \times 1.5\,\mu m^2$ AFM images can be observed that the bigger grain from 0.1 M and 0.2 M NaPSS images are formed by association of small polymeric grain assuring a better coating capacity of polymeric film.

The surface wettability of biocompatible polypyrrole (PPy) films was changed both via surfactant concentration and surface roughness, and we have demonstrated switchable week hydrophilic – strong hydrophilic surfaces, using different concentration of NaPSS.

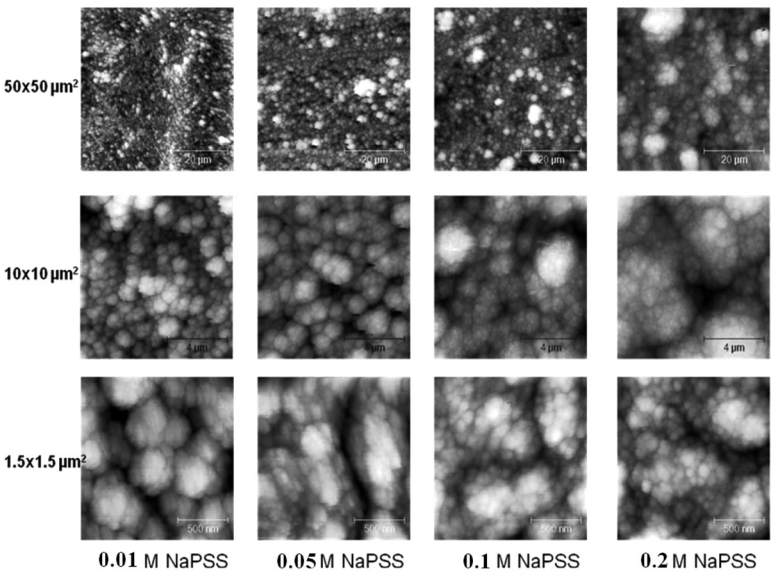

Figure 8. Two-dimensional images of different scans for Polypyrrole/NaPSS in the presence of different concentration of NaPSS.

The roughness parameters obtained from AFM images are presented in the Table 4.

The surfactants increase the roughness values of the PPy/surfactant composite than those corresponding to the PPy film.

Conclusions

The surface wettability of biocompatible polypyrrole (PPy) films was changed both via surfactant concentration and surface roughness, and we have demonstrated switchable week hydrophilic – strong hydrophilic surfaces, using different concentration of NaPSS.

The best anti-corrosion behavior and hydrophilic behavior was observed in case of Ti6Al7Nb/PPy/0.1 mol L^{-1} NaPSS surface, with the contact angle value of about 10.14° comparing with 84° for uncoated titanium alloy.

The concentration of the surfactant plays an important role in the electropolymerisation process assuring a better coating capacity of the composite polymeric film.

A very good stability of PPy composite/titanium alloy surface creates the perspectives of using PPy/NaPSS coatings to sensor and biosensor application.

Acknowledgments

The authors gratefully acknowledge the financial support of the Romanian National CNCSIS Grant IDEI PCCE 248/2008.

References

[1] Balazic, M., Kopac, J., Jackson, M. J., & Ahmed, W. (2007). *International Journal of Nano and Biomaterials*, *1*, 3.
[2] Morra, M. (2006). *European Cells and Materials*, *12*, 1.
[3] Iijima, D., Yoneyama, T., Doi, H., Hamanaka, H., & Kurosaki, N. (2003). *Biomaterials*, *24*, 1519.
[4] Milošev, I., Kosec, T., & Strehblow, H. H. (2008). *Electrochimica Acta*, *53*, 3547.
[5] Tamilselvi, S., Raman, V., & Rajendran, N. (2006). *Electrochimica Acta*, *52*, 839.
[6] Baleani, M., Viceconti, M., & Toni, A. (2000). *Artif. Organs*, *24*(4), 296.
[7] Buser, D., Nydegger, T., Oxland, T., Cochran, D. L., Schenk, R. K., Hirt, H. P., Snetivy, D., & Nole, L. P. (1999). *J. Biomed. Mater. Res.*, *45*, 75–83.
[8] Sprianoa, S., Bosettib, M., Bronzonia, M., Vernea, E., Mainac, G., Bergoc, V., & Cannas, M. (2005). *Biomaterials*, *26*, 1219–1229.
[9] Mindroiu, M., Pirvu, C., Popescu, S., & Demetrescu, I. (2009). *Materiale Plastice*, *46*(4), 394–398.
[10] Kokubo, T., Kim, H. M., & Kawashita, M. (2003). *Biomaterials*, *24*, 2161. 180.
[11] Jonasova, L., Müller, F., Helebrant, A., Strnad, J., & Greil, P. (2002). *Biomaterials*, *23*, 3095.
[12] Mindroiu, V. M., Cicek, E., & Ciubar, R. (2008). *Mol. Cryst. Liq. Cryst.*, *486*, 120 = [1168]–132 = [1180].
[13] Mihaela, M., Miculescu, F., & Demetrescu, I. (2007). *Revista de Chimie.*
[14] Richardson-Burnsa, M. S., Hendricksc, J. L., Fosterd, B., Povlich, L. K., Kimc, D. H., & Martin, D. C. (2007). *Biomaterials*, *28*, 1539.
[15] Guimarda, N. K., Gomezb, N., & Schmidt, C. E. (2007). *Prog. Polym. Sci.*, *32*, 876.
[16] Ateh, D. D., Navsaria, H. A., & Vadgama, P. (2006). *J. R. Soc. Interface*, *3*, 741.

[17] Earley, S. T., Dowling, D. P., Lowry, J. P., & Breslin, C. B. (2005). *Synthetic Metals*, *148*, 111.
[18] Grodz, I. Z., Mista, W., & Strek, W. (2004). *Opt. Mater.*, *26*, 207–212.
[19] Bazzaoui, M., Bazzaoui, E. A., Martins, L., & Martins, J. I. (2002). *Synth. Met.*, *130*, 73–83.
[20] Nguyen, T. L., Garcia, B., Deslouis, C., & Xuan, L. Q. (2002). *J. of Applied Electrochemistry*, *32*, 105–110.
[21] Vatsalarani, J., Geetha, S., Trivedi, D. C., & Warrier, P. C. (2006). *Journal of Power Sources*, *158*, 1484–1489.
[22] Giglio, E. D., De Cennaro, L., Sabbatini, L., & Zambonin, G. (2001). *J. Biomater. Sci. Polym. Ed*, *12*, 63–76.
[23] Rodrigez, L. M. T., Billon, M., Roget, A., & Bidan, G. (2002). *J. Electroanal. Chem*, *523*, 70–78.
[24] Collier, J. H., Camp, J. P., Hudson, T. W., & Schmidt, C. E. (2000). *J. Biomed. Mater. Res.*, *50*, 574–584.
[25] Giglio, E. D., Sabbatini, L., Colucci, S., & Zambonin, G. (2000). *J. Biomater. Sci. Polym. Ed.*, *11*, 1073–1083.
[26] Hien, N. T. L., Garcia, B., Pailleret, A., & Deslouis, C. (2005). *Electrochim. Acta*, *50*, 1747–1755.
[27] Saidman, S. B. & Vela, M. E. (2005). *Thin Solid Films*, *493*, 96–103.
[28] Jun Nie, Tallman, Dennis E., & Bierwagen, Gordon P. (2008). *J. Coat. Technol. Res.*, *5*(3), 327–334.
[29] Aouada, F. A., de Moura, M. R., Radovanovic, E., Girotto, E. M., Rubira, A. F., & Muniz, E. C. (2008). *E-Polymers*, *154*, 1.
[30] George, P. M., Lyckman, A. W., LaVan, D. A., Hegde, A., Leung, Y., Avasare, R., Testa, C., Alexander, P. M., Langer, R., & Sur, M. (2005). *Biomaterials*, *26*, 3511.
[31] Kwokal, A., Piljac, J., & Metikos –Hukovic, M. (2003). *Biomaterials*, *24*, 3765.
[32] De Giglio, E., Guascito, M. R., Sabbatini, L., & Zambonin, G. (2001). *Biomaterials*, *22*, 2609–2616.
[33] Otero, T. F. & Sansiiiena, J. M. (1996). *J. Electroanalytical Chem.*, *412*, 109–116.
[34] Ocon, P., Cristobal, A. B., Herrasti, P., & Fatas E. (2005). *Corrosion Science*, *47*, 649.
[35] Liu, J. & Wan, M. (2001). *J. Mater. Chem.*, *11*, 2022–2027.
[36] Branzoi, V. & Pilan, L. (2008). *Mol. Cryst. Liqu. Cryst.*, *484*, 303–321.
[37] Madden, J. D., Madden, P. G., Anquetil, P. A., & Hunter, I. W. *Proceeding of MRS Fall Meeting 2001*, Vol. 698.
[38] Tilton, R. D., Roberston, C. R., & Gast, A. P. (1991). *Langmuir*, *7*, 2710–2718.
[39] Nakejima, A., Hashimoto, K., & Watanabe, T. (2001). *Monatsh. Chem.*, *132*, 31–41.
[40] Mecerreyes, D., Alvaro, V., Cantero, I., Bengoetxea, M., Calvo, P. A., Grande, H., Rodriguez, J., & Pomposo, J. A. (2002). *Adv. Mater.*, *14*, 749–752.
[41] Isaksson, J., Tengstedt, C., Fahlman, M., Robinson, N., & Berggren, M. (2004). *Adv. Mater.*, *16*, 316–320.
[42] Yee, L. M., Kassim, A., Mahmud, H. N. M. E., Sharif, A. M., & Haron, M. J. (2007). *The Malaysisn Journal of Analytical Sciences*, *11*(133).
[43] Yee, L. M., Mahmud, H. N. M. E., Kassim, A., & Yunus, W. M. M. (2007). *Synthetic Metals*, *157*, 386.
[44] Kassim, A., Mahmud, H. N. M. E., Yee, L. M., & Hanipah, N. (2006). *The Pacific Journal of Science and Technology*, *7*, 103.
[45] Xia, Y. & Lu, Y. (2008). *Composites Science and Technology*, *68*, 1471.
[46] Vishnuvardhan, T. K., Kulkarni, V. R., Basavaraja, C., & Raghavendra, S. C. (2006). *Bull. Mater. Sci.*, *29*, 77.
[47] Hediger, H. J. (1971). *Methoden der Analyse in der Chemie*. Infrarotspektroskopie, Akademische Verlagsgesellschaft: Frankfurt/Main, German.
[48] Lu, X. F., Cao, D. M., Jingyu, C., Zhang, W. J., & Yen, W. (2006). *Mater Lett*, *60*, 2851.